



CHORUS

This is the accepted manuscript made available via CHORUS. The article has been published as:

Phase transitions in the one-dimensional long-range diluted Heisenberg spin glass

Auditya Sharma and A. P. Young

Phys. Rev. B **83**, 214405 — Published 9 June 2011

DOI: [10.1103/PhysRevB.83.214405](https://doi.org/10.1103/PhysRevB.83.214405)

Phase Transitions in the 1-d Long-Range Diluted Heisenberg Spin Glass

Auditya Sharma¹ and A. P. Young^{1,*}

¹*Department of Physics, University of California, Santa Cruz, California 95064*

(Dated: April 25, 2011)

We use Monte Carlo simulations to study the one-dimensional long-range diluted Heisenberg spin glass with interactions that fall as a power, σ , of the distance. Varying the power is argued to be equivalent to varying the space dimension of a short-range model. We are therefore able to study both the mean-field and non-mean-field regimes. For one value of σ , in the non-mean-field regime, we find evidence that the chiral glass transition temperature may be somewhat higher than the spin glass transition temperature. For the other values of σ we see no evidence for this.

PACS numbers: 75.50.Lk, 75.40.Mg, 05.50.+q

I. INTRODUCTION

In the theory of phase transitions it is often helpful to study models in a range of dimensions ranging from above the “upper critical dimension”, d_u , where mean-field critical behavior is expected, to below the “lower critical dimension”, d_l , where fluctuations destroy the transition. However, it has been difficult to do this numerically for spin glasses, since $d_u = 6$ is quite large, and slow dynamics prevents more than a few thousand spins being equilibrated at low temperature T . It follows that, at and above d_u , one cannot study a sufficient range of sizes to perform the necessary finite-size scaling analysis.

As a result, there has been a lot of recent attention on long-range models in one-dimension, in which the interactions fall off with a power of the distance. Such models have a venerable history going back to Dyson^{1,2}, who considered a ferromagnet with interactions falling off like $1/r^\sigma$, and found a paramagnet-ferromagnet transition for $1 < \sigma \leq 2$. Kotliar et al.³ studied the spin glass version of this model, which has received a lot of attention numerically in the last few years⁴⁻⁸.

There are few analytical results on spin glasses beyond mean field theory. For the long-range models, Kotliar et al.³ computed critical exponents in an expansion away from the point where mean field theory occurs (ϵ -expansion), but, as we shall see, this is poorly converged. Hence, most of what we know has come from numerical work. Much of this, including numerics on long-range spin glass models, has studied the Ising version. However, there are also reasons to study models with vector spins, such as the Heisenberg (3-component) model.

One motivation is that Kawamura⁹ proposed that there are two separate transitions in vector spin glasses, a spin glass transition at $T = T_{SG}$ and a “chiral glass transition” at higher temperature T_{CG} , involving a freezing of vortex-like variables called chiralities. While the original scenario had $T_{SG} = 0$, it now appears that T_{SG} is non-zero in three or more dimensions, but the question of whether $T_{SG} < T_{CG}$, or whether there is a single transition at which both types of ordering occur, is still open¹⁰⁻²⁰.

A second motivation for studying the Heisenberg, rather than Ising, spin glass is that it is possible to study larger sizes, see for example Ref.¹⁹, which should be helpful in a finite-size scaling analysis. In a second paper in this series²¹, we will investigate whether there is a de Almeida-Thouless²² (AT) line of transitions in a magnetic field for Heisenberg spin glasses. This follows our recent work²³ which shows that there *is* an AT line for vector spin glasses provided one considers a random field. The ability to study larger sizes will be particularly useful for the AT-line study.

Here we present data for the zero field transition for the Heisenberg spin glass for values of the parameter σ corresponding to (i) the mean-field regime, (ii) the non-mean-field regime, and (iii) the borderline case where the transition disappears. Most of our results find no evidence for separate spin-glass and chiral-glass transitions. However, for one set of parameters in the non-mean-field regime, the data indicates that T_{CG} may be somewhat greater than T_{SG} . Whether this result remains valid in the thermodynamic limit, will require future studies on significantly larger systems.

The plan of this paper is as follows. In Sec. II we describe the model that we study, while in Sec. III we give some technical details of the simulations. The results are presented in Sec. IV and our conclusions summarized in Sec. V.

II. MODEL

We consider the Hamiltonian

$$\mathcal{H} = - \sum_{\langle i,j \rangle} J_{ij} \mathbf{S}_i \cdot \mathbf{S}_j, \quad (1)$$

where \mathbf{S}_i are classical 3-component Heisenberg spins of length 1, and the interactions J_{ij} are independent variables with zero mean and a variance which falls off with a power of the distance between the spins,

$$[J_{ij}^2]_{av} \propto \frac{1}{r_{ij}^{2\sigma}}, \quad (2)$$

where $[\dots]_{av}$ means an average over disorder. In the version used in early studies⁴, every spin interacts with

every other spin with a strength which falls off, on average, like Eq. (2). However, this means that the CPU time per sweep varies as N^2 , rather than N , so large sizes can not be studied. This problem was solved by Leuzzi et. al.⁶ who proposed a model in which, instead of the *magnitude* of the interaction falling off with distance like Eq. (2), it is the *probability* of there being a non-zero interaction between sites (i, j) which falls off, and when an interaction does exist, its variance is independent of r_{ij} . The mean number of non-zero interactions from a site, which we call z , can be fixed, and we take $z = 6$. To generate the set of pairs (i, j) that have an interaction with the desired probability we choose spin i randomly, and then choose j ($\neq i$) at distance r_{ij} with probability

$$p_{ij} = \frac{r_{ij}^{-2\sigma}}{\sum_{j(j\neq i)} r_{ij}^{-2\sigma}}, \quad (3)$$

where, for r_{ij} , we put the sites on a circle and use the distance of the chord, i.e.

$$r_{ij} = \frac{N}{\pi} \sin \left[\frac{\pi}{N} (i - j) \right]. \quad (4)$$

If i and j are already connected, we repeat the process until we find a pair which has not been connected before. We then connect i and j with an interaction picked from a Gaussian interaction whose mean is zero and whose standard deviation is J , which set equal to 1. This process is repeated precisely $N_b = zN/2$ times.

The result is that each pair (i, j) will be connected with a probability P_{ij} which must satisfy the condition $N \sum_j P_{ij} = Nz$ since P_{ij} only depends on $|i - j|$, $P_{ii} = 0$, and there are precisely $Nz/2$ connected pairs. It follows that, for a fixed site i ,

$$\sum_j [J_{ij}^2]_{av} = J^2 \sum_j P_{ij} = J^2 z. \quad (5)$$

Note that P_{ij} is different from $z \times p_{ij}$ in Eq. (3) because of the constraint that no bond can occur twice. The mean-field spin glass transition temperature for m -component vector spins is given by²⁴

$$T_{SG}^{MF} = \frac{1}{m} \left(\sum_j [J_{ij}^2]_{av} \right)^{1/2} = \frac{\sqrt{z}}{m} J, \quad (6)$$

where the last equality follows from Eq. (5). We set $J = 1$ so that, for the situation here,

$$J = 1, \quad z = 6, \quad m = 3, \quad (7)$$

we have

$$T_{SG}^{MF} = \frac{\sqrt{6}}{3} \simeq 0.816, \quad (8)$$

the same as for the nearest-neighbor Heisenberg spin glass on a simple cubic lattice.

TABLE I: A summary of the behavior for different ranges of σ in one space dimension and at zero field. Infinite range means that $\sum_{j(j\neq i)} J_{ij}^2$ diverges unless the bonds J_{ij} are scaled by an inverse power of the system size. The behavior is mean-field like for $\sigma < \sigma_u$ where $\sigma_u = 2/3$, and a finite-temperature transition no longer occurs for $\sigma > \sigma_l$ where $\sigma_l = 1$.

σ	Behavior
$\sigma = 0$	SK model
$0 < \sigma \leq 1/2$	Infinite range
$1/2 < \sigma < 2/3$	Mean-field with $T_{SG} > 0$
$2/3 < \sigma \leq 1$	Non-mean-field with $T_{SG} > 0$
$1 < \sigma$	$T_{SG} = 0$

By varying σ one finds different types of behavior^{3,25}, as shown in Table I. For $\sigma < 1/2$ the model is non-extensive (for instance the mean-field transition temperature in Eq. (6) diverges) unless the interactions are scaled by an inverse power of the system size. We will call this “infinite range”. The extreme limit of this, $\sigma = 0$, is the Sherrington-Kirkpatrick²⁶ model, whose exact solution was found by Parisi²⁷⁻²⁹. In fact, it has been suggested³⁰ (see also Ref. 31) that, in the thermodynamic limit, the behavior of the model is *identical* to that of the SK model for the *whole range* $0 \leq \sigma < 1/2$.

The model is extensive for $\sigma > 1/2$ and a finite temperature transition is expected for $\sigma < \sigma_l$, where the “lower critical” value is

$$\sigma_l = 1. \quad (9)$$

The transition is in the mean-field universality class³ for $\sigma < \sigma_u$, where the “upper critical” value is

$$\sigma_u = 2/3. \quad (10)$$

For $\sigma_u < \sigma < \sigma_l$, there is a finite-temperature transition with non mean-field critical exponents. In this paper we will study both mean-field and non mean-field regions. Finally for $\sigma > \sigma_l$ there is no transition at finite temperature.

III. NUMERICAL SETUP

We perform large scale Monte-Carlo simulations for $\sigma = 0.6, 0.75, 0.85$ and 1. From the previous section we note that $\sigma = 0.60$ is in the mean-field regime, $\sigma = 0.75$ and 0.85 are in the non mean-field regime, and $\sigma = 1$ is the borderline case, $\sigma = \sigma_l$, beyond which there is no transition. A plausible scenario is that $T_{SG} = 0$ for $\sigma = 1$, though the possibility that T_{SG} is non-zero cannot be ruled out *a priori*. Table II lists the parameters of the simulation.

A. Equilibration

As discussed in earlier work^{5,32} there is a convenient test for equilibration with Gaussian interactions, namely

TABLE II: Parameters of the simulations. N_{samp} is the number of samples, N_{equil} is the number of overrelaxation Monte Carlo sweeps for equilibration for each of the $2N_T$ replicas for a single sample. The same number of sweeps is done in the measurement phase, with a measurement performed every four overrelaxation sweeps. The number of heatbath sweeps is equal to 10% of the number of overrelaxation sweeps. T_{min} and T_{max} are the lowest and highest temperatures simulated, and N_T is the number of temperatures used in the parallel tempering.

σ	N	N_{samp}	N_{equil}	T_{min}	T_{max}	N_T
0.6	128	16000	128	0.20	0.70	40
0.6	256	16000	256	0.20	0.70	40
0.6	512	16000	512	0.20	0.70	40
0.6	1024	16000	1024	0.20	0.70	40
0.6	2048	16000	2048	0.20	0.70	40
0.6	4096	6100	4096	0.30	0.70	40
0.6	8192	1000	8192	0.30	0.70	50
0.6	16384	500	16384	0.35	0.70	55
0.6	32768	400	32768	0.35	0.70	60
0.75	128	8000	128	0.20	0.55	40
0.75	256	8000	256	0.20	0.55	40
0.75	512	8000	512	0.20	0.55	40
0.75	1024	3000	1024	0.20	0.55	40
0.75	2048	3000	2048	0.20	0.55	40
0.75	4096	3000	4096	0.20	0.55	40
0.75	8192	1100	8192	0.20	0.55	50
0.75	16384	500	16384	0.25	0.55	55
0.75	32768	400	32768	0.25	0.55	60
0.85	128	16000	512	0.09	0.30	40
0.85	256	16000	1024	0.09	0.30	40
0.85	512	10000	2048	0.09	0.30	40
0.85	1024	10000	8192	0.14	0.22	20
0.85	2048	8000	16384	0.14	0.22	20
0.85	4096	4000	32768	0.14	0.22	36
0.85	8192	2000	65536	0.15	0.21	20
0.85	16384	1700	131072	0.16	0.21	20
1.0	128	2000	2048	0.03	0.10	10
1.0	256	2000	4096	0.03	0.10	10
1.0	512	2000	16384	0.02	0.10	40
1.0	1024	1200	524288	0.017	0.08	40
1.0	2048	500	2097152	0.017	0.08	60

the relationship

$$U = \frac{J^2}{T} \frac{z}{2} (q_l - q_s), \quad (11)$$

is valid in equilibrium but the two sides approach their common equilibrium value from opposite directions as equilibrium is approached. Here $U = -(1/N) [\sum_{\langle i,j \rangle} \epsilon_{ij} J_{ij} \langle \mathbf{S}_i \cdot \mathbf{S}_j \rangle]_{\text{av}}$ is the average energy per spin, $q_l = (1/N_b) \sum_{\langle i,j \rangle} \epsilon_{ij} [(\mathbf{S}_i \cdot \mathbf{S}_j)^2]_{\text{av}}$ is the “link overlap”, and $q_s = (1/N_b) \sum_{\langle i,j \rangle} \epsilon_{ij} [(\langle \mathbf{S}_i \cdot \mathbf{S}_j \rangle)^2]_{\text{av}}$, where $N_b = zN/2$, and $\epsilon_{ij} = 1$ if there is a bond between i and j and is zero otherwise. Equation (11) is easily derived by integrating by parts the expression for the average energy with respect to J_{ij} since it has a Gaussian distribution. Note that in the numerics we set $J = 1$.

We determine both sides of Eq. (11) for different num-

bers of Monte Carlo sweeps (MCS) which increase in a logarithmic manner, each value being twice the previous one. In all cases we average over the last half of the sweeps. We consider the data to be equilibrated, if, when averaging over a large number of samples, Eq. (11) is satisfied for at least the last two points.

B. Simulation Technology

To equilibrate the system in as small a number of sweeps as possible, with the minimum amount of CPU time, we perform three types of Monte Carlo sweeps^{17–19}.

The workhouse of our simulation is the “Microcanonical” sweep³³ (also known as an “over-relaxation” sweep). We sweep sequentially through the lattice, and, at each site, compute the local field on the spin, $\mathbf{H}_i = \sum_j J_{ij} \mathbf{S}_j$. The new value for the spin on site i is taken to be its old value reflected about \mathbf{H} , i.e.

$$\mathbf{S}'_i = -\mathbf{S}_i + 2 \frac{\mathbf{S}_i \cdot \mathbf{H}_i}{H_i^2} \mathbf{H}_i. \quad (12)$$

These sweeps are microcanonical because they preserve energy. They are very fast because the operations are simple and no random numbers are needed. For reasons that are not fully understood, it also seems that they “stir up” the spin configuration very efficiently¹⁸ and the system equilibrates faster than if one only uses “heatbath” updates, described next, see e.g. Fig. 9 of Ref. [34].

We also need to do “Heatbath” sweeps in order to change the energy. As for the microcanonical case, we sweep sequentially through the lattice. We take the direction of the local field \mathbf{H}_i , to be the polar axis for the spin on site i . We compute the polar and azimuthal angle of the new spin direction relative to the local field by the requirement that this direction occurs with the Boltzmann probability, see Ref. [17] for details.

Finally we perform parallel tempering sweeps^{35,36} to prevent the system from being trapped in local minima at low temperature. We take N_T copies of the system with the same bonds but at a range of different temperatures. The minimum temperature, $T_{\text{min}} \equiv T_1$, is the low temperature where one wants to investigate the system (below T_{SG} in our case), and the maximum, $T_{\text{max}} \equiv T_{N_T}$, is high enough that the the system equilibrates very fast (well above T_{SG} in our case). A parallel tempering sweep consists of swapping the temperatures of the spin configurations at a pair of neighboring temperatures, T_i and T_{i+1} , for $i = 1, 2, \dots, T_{N_T-1}$ with a probability that satisfies the detailed balance condition. The Metropolis probability for this is³⁵

$$P(T \text{ swap}) = \begin{cases} \exp(\Delta\beta \Delta E), & (\text{if } \Delta\beta \Delta E > 0), \\ 1, & (\text{otherwise}), \end{cases} \quad (13)$$

where $\Delta\beta = 1/T_i - 1/T_{i+1}$ and $\Delta E = E_i - E_{i+1}$, in which E_i is the energy of the copy at temperature T_i . In this

way, a given set of spins (i.e. a copy) performs a random walk in temperature space.

We perform one parallel tempering sweep for every ten overrelaxation sweeps. Since there are two copies of spins *at each temperature*, indicated by labels “(1)” and “(2)” in Eq. (14) below, we actually perform parallel tempering sweeps among the set of N_T copies labeled “(1)” and, separately, among the set of N_T copies labeled “(2)”.

C. Quantities Measured

The main quantities measured in this simulation are the spin glass susceptibility χ_{SG} , and the chiral glass susceptibility χ_{CG} , at wavevectors $k = 0$, and $k = 2\pi/N$, and from these we obtain the two corresponding correlation lengths, ξ_{SG} and ξ_{CG} . The spin glass order parameter, $q^{\mu\nu}(k)$, at wave vector k , is defined to be

$$q^{\mu\nu}(k) = \frac{1}{N} \sum_{i=1}^N S_i^{\mu(1)} S_i^{\nu(2)} e^{ik \cdot R_i}, \quad (14)$$

where μ and ν are spin components, and “(1)” and “(2)” denote two identical copies of the system with the same interactions. We run two copies of the system at each temperature in order to evaluate quantities such as the spin glass susceptibility, defined in Eq. (15) below, without bias. From this we determine the wave vector dependent spin glass susceptibility $\chi_{SG}(k)$ by

$$\chi_{SG}(k) = N \sum_{\mu,\nu} [\langle |q^{\mu\nu}(k)|^2 \rangle]_{\text{av}}, \quad (15)$$

where $\langle \dots \rangle$ denotes a thermal average and $[\dots]_{\text{av}}$ denotes an average over disorder. The spin glass correlation length is then determined from

$$\xi_{SG} = \frac{1}{2 \sin(k_{\min}/2)} \left(\frac{\chi_{SG}(0)}{\chi_{SG}(k_{\min})} - 1 \right)^{1/(2\sigma-1)}, \quad (16)$$

where $k_{\min} = (2\pi/L)$. For the Heisenberg spin glass, Kawamura defines the local chirality in terms of three spins on a line as follows¹⁰:

$$\kappa_i = \mathbf{S}_{i+1} \cdot \mathbf{S}_i \times \mathbf{S}_{i-1}. \quad (17)$$

The chiral glass susceptibility is then given by

$$\chi_{CG}(k) = N [\langle |q_c(k)|^2 \rangle]_{\text{av}}, \quad (18)$$

where the chiral overlap $q_c(\mathbf{k})$ is given by

$$q_c(k) = \frac{1}{N} \sum_{i=1}^N \kappa_i^{(1)} \kappa_i^{(2)} e^{ik \cdot R_i}. \quad (19)$$

We define the chiral correlation length by

$$\xi_{CG} = \frac{1}{2 \sin(k_{\min}/2)} \left(\frac{\chi_{CG}(0)}{\chi_{CG}(k_{\min})} - 1 \right)^{1/(2\sigma-1)}. \quad (20)$$

As will be revealed in the next section, three of the four quantities defined above, χ_{SG} , ξ_{SG} , and χ_{CG} may be used in a finite-size-scaling analysis to locate and analyze the phase transition.

D. Finite-Size Scaling

According to finite-size scaling³⁷, the correlation length of the finite-system varies, near the transition temperature T_c , as

$$\frac{\xi}{N} = \mathcal{X}[N^{1/\nu}(T - T_c)], \quad (2/3 \leq \sigma < 1), \quad (21a)$$

$$\frac{\xi}{N^{\nu/3}} = \mathcal{X}[N^{1/3}(T - T_c)], \quad (1/2 < \sigma \leq 2/3), \quad (21b)$$

in which ν , the correlation length exponent, is given, in the mean-field regime, by $\nu = 1/(2\sigma - 1)$. We will use Eq. (21) for both the spin glass correlation length ξ_{SG} , in which T_c will be set to T_{SG} , and the chiral glass correlation length ξ_{CG} , in which T_c will be set to T_{CG} . It follows that, if there is a transition at $T = T_c$, data for ξ/N ($\xi/N^{\nu/3}$ in the mean-field region) for different system sizes N should cross at T_c .

We also present data for $\chi_{SG} \equiv \chi_{SG}(0)$, which has the finite-size scaling form

$$\frac{\chi_{SG}}{N^{2-\eta}} = \mathcal{C}[N^{1/\nu}(T - T_c)], \quad (2/3 \leq \sigma < 1), \quad (22a)$$

$$\frac{\chi_{SG}}{N^{1/3}} = \mathcal{C}[N^{1/3}(T - T_c)], \quad (1/2 < \sigma \leq 2/3). \quad (22b)$$

Hence curves of $\chi_{SG}/N^{2-\eta}$ ($\chi_{SG}/N^{1/3}$ in the mean-field regime) should also intersect. This is particularly useful for long-range models since η is given by the simple expression $2 - \eta = 2\sigma - 1$ *exactly*. However, we do not know the exponent corresponding to η for the chiral glass susceptibility, so we will not use this quantity in the finite-size scaling analysis.

In practice, there are corrections to this finite-size-scaling, so data for different sizes do not all intersect at the exactly the same temperature. Including leading corrections to scaling, the intersection temperature $T^*(N, 2N)$ for sizes N and $2N$ varies as³⁸⁻⁴¹

$$T^*(N, 2N) = T_c + \frac{A}{N^\lambda}, \quad (23)$$

where A is the amplitude of the leading correction, and the exponent λ is given by

$$\lambda = \frac{1}{\nu} + \omega \quad (24)$$

where ω is the leading correction to scaling exponent.

IV. RESULTS

A. $\sigma = 0.6$ (mean-field regime)

As shown in Table I, $\sigma = 0.6$ lies well inside the mean-field regime. Hence, according to Eq. (21b), results for $\xi_{SG}/N^{\nu/3}$ should intersect at T_{SG} with ν set equal to $1/(2\sigma - 1)$. The data is shown in the main part of

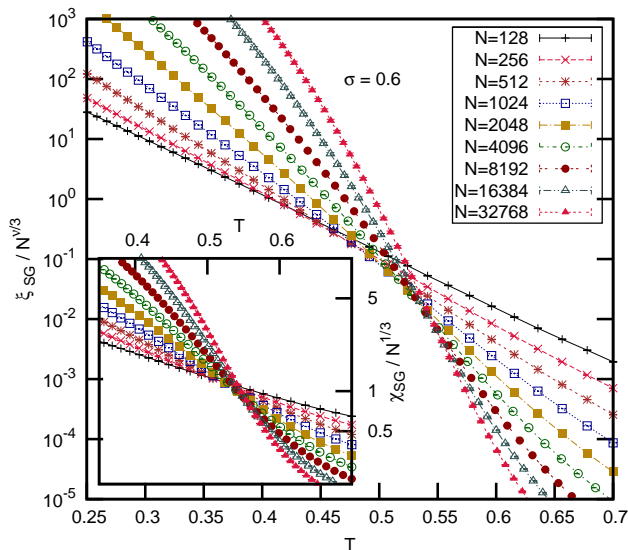


FIG. 1: (Color online) The main figure shows data for $\xi_{SG}/N^{5/3}$, in which the power of N is chosen following Eq. (21b) with $\nu = 1/(2\sigma - 1)$, as a function of T for different system sizes for $\sigma = 0.6$. The inset shows data for $\chi_{SG}/N^{1/3}$, in which the power of N is chosen following Eq. (22b).

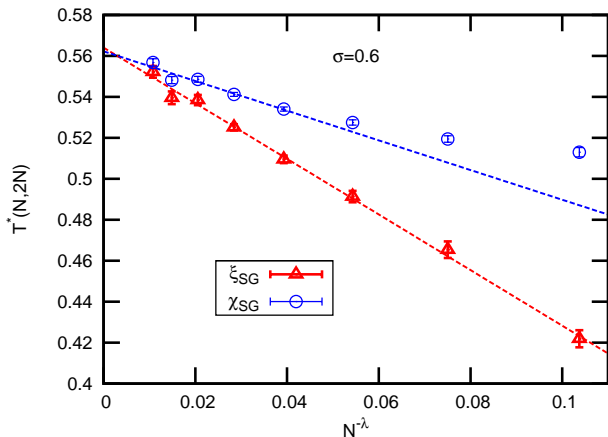


FIG. 2: (Color online) The intersection temperatures, $T^*(N, 2N)$, obtained from the data in Fig. 1, for $\xi_{SG}/N^{5/3}$ and $\chi_{SG}/N^{1/3}$ for $\sigma = 0.6$, as a function of $N^{-\lambda}$, with $\lambda = 0.467$ determined from Eq. (24) (which is valid in the MF regime). A fit using all 8 points from ξ_{SG} gives $T_{SG} = 0.564 \pm 0.002$, while a fit using the data for the largest 5 pairs of sizes from χ_{SG} gives $T_{SG} = 0.562 \pm 0.002$.

Fig. 1. The intersections do not occur at precisely the same temperature, but fitting the intersection temperatures to Eq. (23) is helped by the fact that we know $\lambda \equiv \frac{5}{3} - 2\sigma$ in the MF regime⁴¹, which gives a value 0.467 here. A straight line fit of $\xi_{SG}/N^{5/3}$ against $N^{-\lambda}$, shown in Fig. 2, gives $T_{SG} = 0.564 \pm 0.002$.

The inset to Fig. 1 shows data for $\chi_{SG}/N^{1/3}$, which

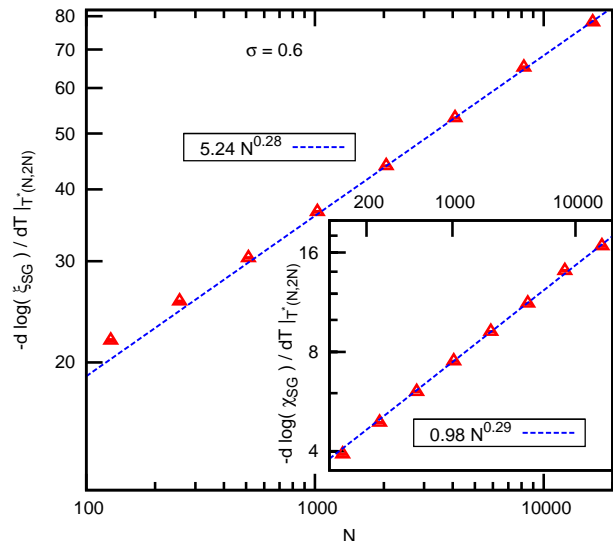


FIG. 3: (Color online) The main figure is a log-log plot of the logarithmic derivative of ξ_{SG} for $\sigma = 0.6$ for different sizes N evaluated at the intersection temperatures $T^*(N, 2N)$ shown in Fig. 2. According to Eq. (21b) the slope is expected to be $1/3$. The best fit is a little smaller than this, indicating that corrections to scaling are still present for these sizes. The inset is the same but for χ_{SG} .

should also intersect at T_{SG} according to Eq. (22b). This time, we find that corrections to scaling are well described Eq. (23) but only if we consider just the largest five pairs of sizes. The fit to Eq. (23), shown in Fig. 2, gives $T_{SG} = 0.562 \pm 0.002$, which is consistent with that obtained from the spin glass correlation length.

We have also measured the chiral glass correlation length. However, we find that $\xi_{CG}/N^{\nu/3} \lesssim 10^{-12}$ in the vicinity of T_{SG} . Hence chiralities can not play an important role in this range of temperature.

According to Eqs. (21b) and (22b) the argument of the scaling functions is $N^{1/3}(T - T_c)$. Hence, at T_{SG} the logarithmic derivative of ξ_{SG} and χ_{SG} should vary as $N^{1/3}$. As we have seen, the data do not all intersect at the same temperature, and so we evaluate the derivatives at the intersection temperatures T^* plotted in Fig. 2. The results are shown in Fig. 3. We get a power of 0.28 from ξ_{SG} and 0.29 from χ_{SG} , in both cases a little less than $1/3$, indicating that there are still some corrections to scaling even for these large sizes.

B. $\sigma = 0.75$ (non mean-field regime)

For $\sigma = 0.75$ we are no longer in the MF regime. Hence, according to Eqs. (21a) and (22a), ξ_{SG}/N and $\chi_{SG}/N^{2-\eta}$ (with $2 - \eta = 2\sigma - 1$), should intersect at T_{SG} . The data are shown in Fig. 4.

We fit the intersection temperatures to Eq. (23), but unfortunately we do not know the value of the exponent

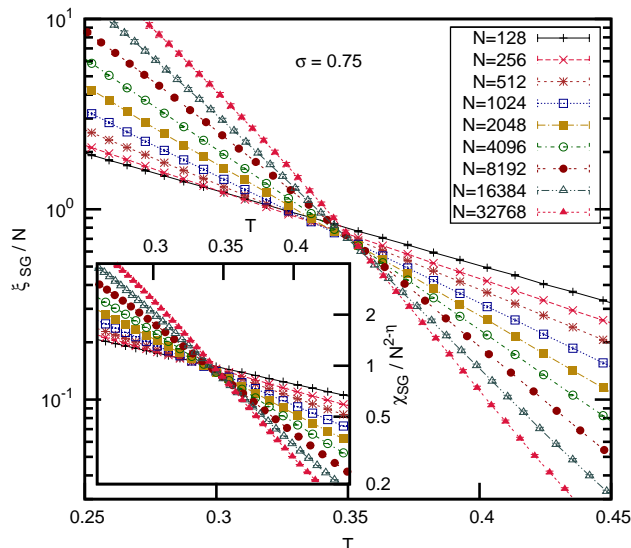


FIG. 4: (Color online) The main figure shows data for different sizes for ξ_{SG}/N at $\sigma = 0.75$ which, according to Eq. (21a), should intersect at T_{SG} . The inset shows data for $\chi_{SG}/N^{2-\eta}$ (with $2 - \eta = 2\sigma - 1$), which should also intersect at T_{SG} according to Eq. (22a).

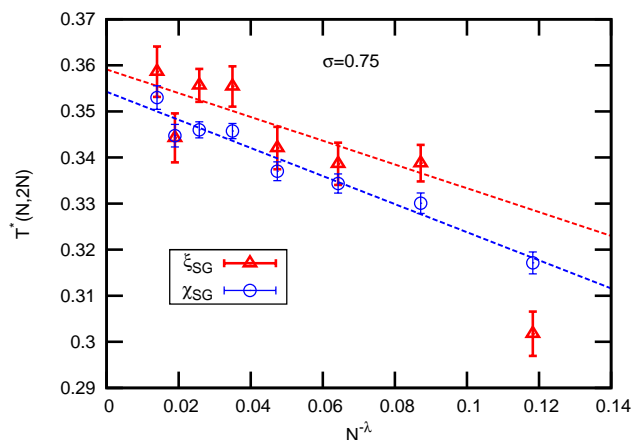


FIG. 5: (Color online) The intersection temperatures for $\sigma = 0.75$. The all 8 data points from χ_{SG} were fitted to Eq. (23), with the result that $\lambda = 0.44 \pm 0.13$. The same exponent was then used to fit the results for the largest 7 (pairs of) sizes from ξ_{SG} , for which sub-leading corrections to scaling seem to be more important. The resulting values for the transition temperature are $T_{SG} = 0.354 \pm 0.005$ from χ_{SG} , and $T_{SG} = 0.359 \pm 0.003$ from ξ_{SG} .

λ outside the MF region, and have to include it as fit parameter. The fit is therefore to a non-linear function of the parameters. We determine the fit parameters using the Levenberg-Marquardt algorithm⁴². The data from χ_{SG} is better behaved than the data from ξ_{SG} so we use the former to determine the exponent λ and then fix this value in the fit (which did not include the smallest size)

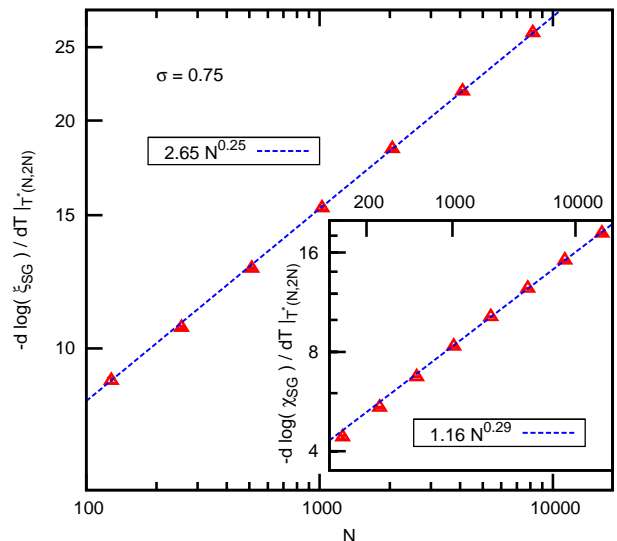


FIG. 6: (Color online) The main figure is a log-log plot of the logarithmic derivative of ξ_{SG} for $\sigma = 0.75$ for different sizes N evaluated at the intersection temperatures $T^*(N, 2N)$ shown in Fig. 5. According to Eq. (21a) the slope is expected to be $1/\nu$. The inset is the same but for χ_{SG} .

to the data from ξ_{SG} . This procedure is justified since the exponent giving the leading correction to scaling, λ , is universal, though the amplitude of this correction (A in Eq. (23)) is non-universal. The results are $\lambda = 0.44 \pm 0.13$, $T_{SG} = 0.359 \pm 0.003$ from ξ_{SG} , and $T_{SG} = 0.354 \pm 0.005$ from χ_{SG} . The two estimates for T_{SG} agree within the error bars.

The data for ξ_{CG}/N in the region of the spin glass transition temperature is very small, around 10^{-4} . Hence, as for $\sigma = 0.6$, chiralities do not play an important role in the transition.

According to Eqs. (21a) and (22a), adapted to include corrections to finite-size scaling, the logarithmic derivative of ξ_{SG} and χ_{SG} should vary as $N^{1/\nu}$ at $T^*(N, 2N)$. The plots in Fig. 6 yield $1/\nu_{SG} = 0.25$ from ξ_{SG} and 0.29 from χ_{SG} . The difference presumably comes from corrections to scaling.

Kotliar et al.³ calculated critical exponents to leading order in $\epsilon = \sigma - 2/3$ with the result

$$\frac{1}{\nu} = \frac{1}{3} (1 - 12\epsilon + O(\epsilon^2)). \quad (25)$$

The large coefficient of ϵ indicates the expansion becomes poorly converged well before the “lower critical” value $\epsilon = 1/3$ ($\sigma = 1$). Even for the present value of σ , which corresponds to $\epsilon = 1/12$, Eq. (25) gives $1/\nu = 0$, and so is not useful for comparison with the numerics.

C. $\sigma = 0.85$ (non mean-field regime)

For $\sigma = 0.85$ we are further in the non-mean-field region. Among the different models studied here, this is

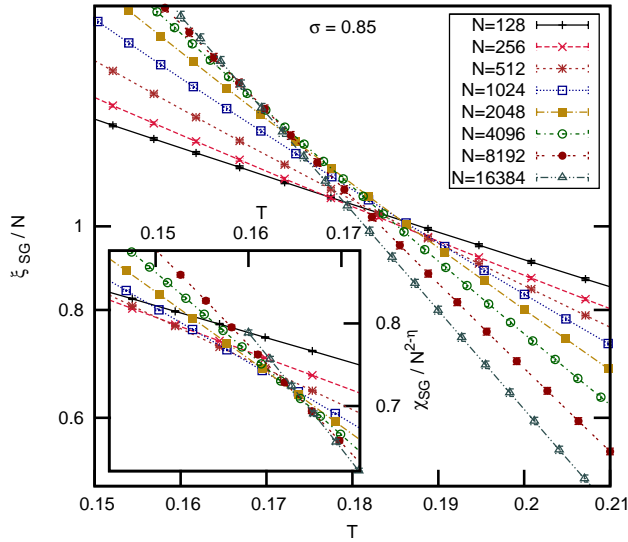


FIG. 7: (Color online) The main figure shows data for ξ_{SG}/N , as a function of T for different system sizes for $\sigma = 0.85$. The inset shows data for $\chi_{SG}/N^{2-\eta}$ with $2-\eta = 2\sigma - 1$.

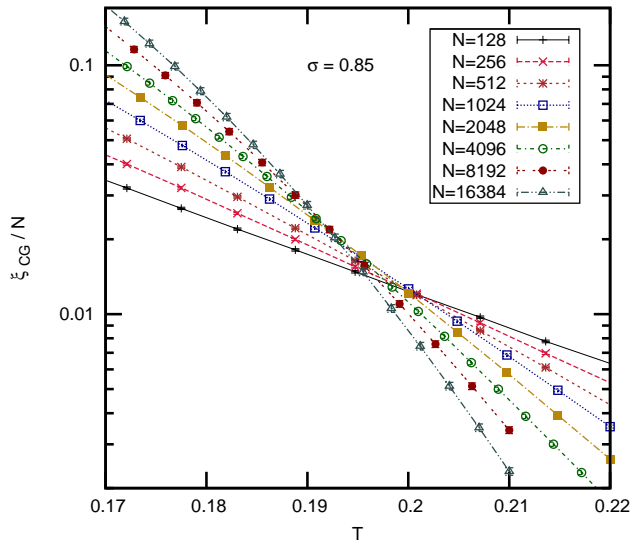


FIG. 8: (Color online) Data for ξ_{CG}/N , the spin glass correlation length divided by system size, as a function of T for different system sizes for $\sigma = 0.85$.

the one which is most similar to a short-range model in three dimensions. The spin glass data is shown in Fig. 7. Chiral correlations are larger than for $\sigma = 0.6$ and 0.75 , so we show data for ξ_{CG} in Fig. 8.

As for $\sigma = 0.75$, to extrapolate the intersection temperatures to the thermodynamic limit, we resort to Levenberg-Marquardt fits with three parameters. Using data from χ_{SG} we find $\lambda_{SG} = 0.99 \pm 0.13$. The data from ξ_{CG} is insufficient to determine λ_{CG} since the fits give $\lambda_{CG} = 0.79 \pm 0.74$, i.e. the error bar is as large as

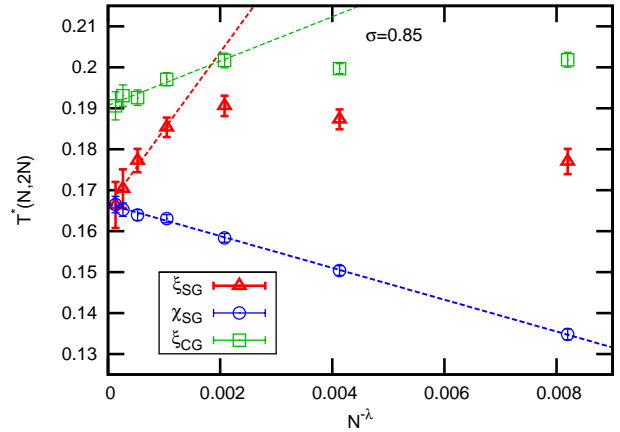


FIG. 9: (Color online) The intersection temperatures for $\sigma = 0.85$. The data from χ_{SG} was fitted to Eq. (23), with the result that $\lambda = 0.99 \pm 0.13$. This is the value used to plot all the data. The same exponent was then used to fit the largest four sizes in the data from ξ_{SG} , for which sub-leading corrections appear to be very large. The full Levenberg-Marquardt fit to the data for ξ_{CG} was unable to determine λ with any precision, see text. However, in estimating T_{CG} and its error bar from data for ξ_{CG} we allowed λ to vary. The resulting values for the transition temperatures are $T_{SG} = 0.167 \pm 0.001$ from χ_{SG} (all 7 points), $T_{SG} = 0.166 \pm 0.004$ from ξ_{SG} (4 points), and $T_{CG} = 0.190 \pm 0.006$ from ξ_{CG} (5 points). We emphasize that, in these estimates, we fixed the value of λ only for the data from ξ_{SG} .

the best estimate. Nonetheless, in estimating T_{CG} and its error bar from the data for χ_{CG} , we allow λ to vary. For ξ_{SG} there appear to be very large sub-leading corrections, so we fixed the value of λ_{SG} to that obtained from χ_{SG} when fitting the results from ξ_{SG} .

Results for $T^*(N, 2N)$ against $1/N^\lambda$ and fits are shown in Fig. 9. In the *plot*, for all data we use the value of λ determined from χ_{SG} . However, we again emphasize that, in the *fit* to the χ_{CG} data, we estimated T_{CG} and its error bar by allowing λ to vary. From the fits, we find $T_{SG} = 0.167 \pm 0.001$ from χ_{SG} , $T_{SG} = 0.166 \pm 0.004$ from ξ_{SG} , and $T_{CG} = 0.190 \pm 0.006$ from ξ_{CG} .

The two estimates of T_{SG} agree with each other but are lower than T_{CG} . This would imply spin-chirality decoupling for $\sigma = 0.85$. However, we note that the data for the spin glass correlation length appears, at intermediate sizes, to be extrapolating to a value for T_{SG} of around 0.19 (our value for T_{CG}) but then, for the largest sizes, veers down to about 0.167 (very close to our value for T_{SG} obtained from χ_{SG}). Hence we cannot rule out the possibility that a similar “crossover” may occur for the chiral glass correlation length data, but at even larger sizes. If so, then spin-chirality decoupling would not occur at the largest scales. We also note that the actual values of ξ_{CG}/N shown in Fig. 8 are still very small in the vicinity of T_{CG} , about 1/50 of the value of ξ_{SG}/N around the transition, see Fig. 7. Hence we are very far

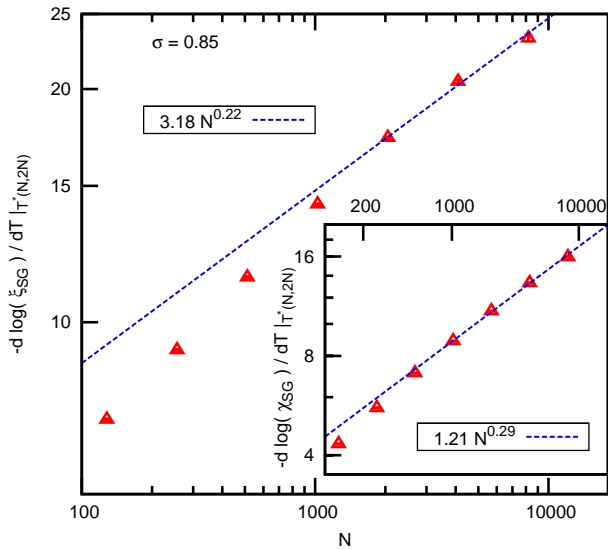


FIG. 10: (Color online) The main figure is a log-log plot of the logarithmic derivative of ξ_{SG} for $\sigma = 0.85$ for different sizes N evaluated at the intersection temperatures $T^*(N, 2N)$ shown in Fig. 9. According to Eq. (21a) the slope is expected to be $1/\nu$. The inset is the same but for χ_{SG} .

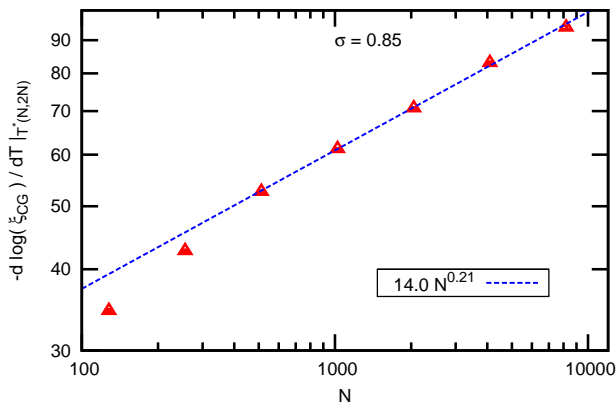


FIG. 11: (Color online) Similar to Fig. 10 but for ξ_{CG} .

the regime with $\xi_{CG} > \xi_{SG}$ which will ultimately occur in the presence of spin-chirality decoupling.

Figure 10 shows results for the logarithmic derivative of ξ_{SG} and χ_{SG} evaluated at $T^*(N, 2N)$. Fits give $1/\nu = 0.22$ from ξ_{SG} and 0.29 from χ_{SG} . The curvature in the data for ξ_{SG} indicates strong finite-size corrections. Presumably these corrections are also the reason for the difference between the two estimates for $1/\nu$. Figure 11 shows similar data but for ξ_{CG} . The best fit gives $1/\nu = 0.21$, which is close to the estimate from ξ_{SG} . Note that the coefficient of $N^{1/\nu}$, 14.01 , is much larger than the corresponding value, 3.18 , for ξ_{SG} , presumably to compensate for the overall value of ξ_{CG} being much less than that of ξ_{SG} in the vicinity of the intersection temperatures T^* .

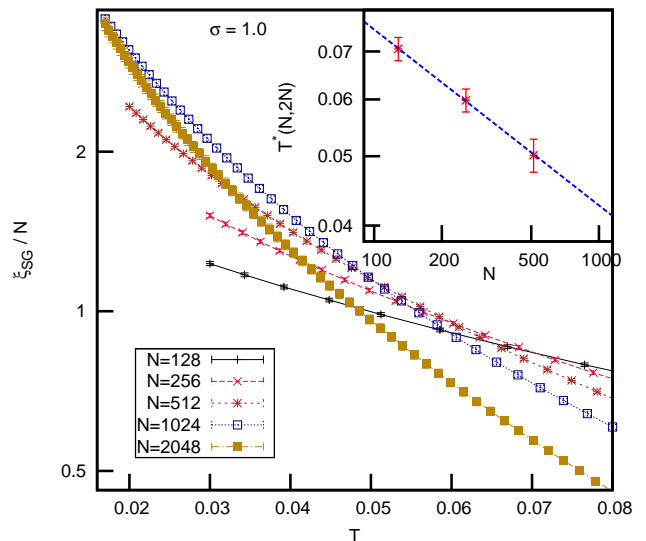


FIG. 12: (Color online) Data for ξ_{SG}/N , the spin glass correlation length divided by system size, as a function of T for different system sizes, for $\sigma = 1.0$. The inset shows the intersection temperatures $T^*(N, 2N)$, as well as a log-log fit assuming $T_{SG} = 0$. The fit works well for $N = 128, 256$ and 512 . There is no intersection for the two lowest sizes, $N = 1024$ and 2048 for T greater than the lowest temperature we could simulate, 0.017 . This temperature is well *below* the value of the fit extrapolated to $N = 1024$, which is about 0.042 . Hence the intersection temperatures actually fall off *faster* at large sizes than shown in the fit.

D. $\sigma = 1$ ($= \sigma_l$)

It is known from the early work of Kotliar et al.³ that $\sigma = 1$ is the “lower critical” value σ_l , above which there is no spin glass transition. Interestingly, Viet and Kawamura²⁰ claim that chiral glass ordering persists to slightly *larger* values of σ . Testing this claim is one of our main motivations for performing simulations at $\sigma = 1$.

Figure 12 shows the finite scaling for ξ_{SG} . In the inset, we show a log-log plot of $T^*(N, 2N)$ versus N and include a straight-line fit for $N = 128, 256$ and 512 . This fit works well. We find no intersections in the range of T that we can equilibrate ($T \geq 0.17$) for $N = 1024$ and 2048 . Hence the data is well consistent with $T_{SG} = 0$.

Figure 13 shows the corresponding figure for ξ_{CG} . Again, the inset shows log-log fits assuming that the transition temperature, T_{CG} in this case, is zero. The fit is satisfactory and indicates that we do not find a finite value for T_{CG} at $\sigma = 1$, in contrast to the claim of Viet and Kawamura²⁰.

Figure 14 shows the data for χ_{SG} . There are no intersections at all in the range of temperature that we can equilibrate, consistent with the conclusion from the ξ_{SG} data that $T_{SG} = 0$.

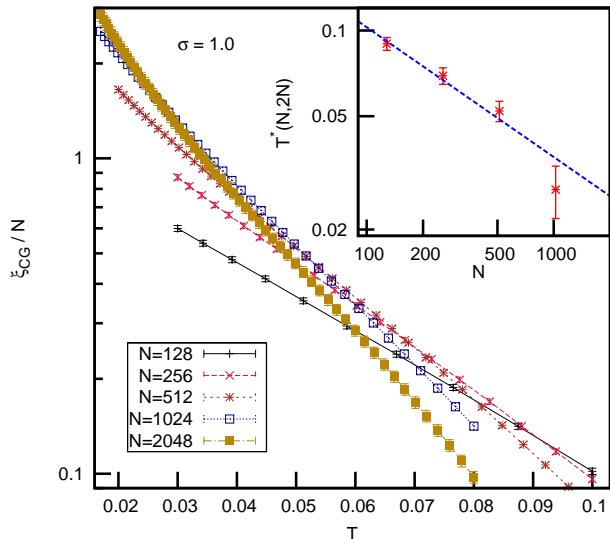


FIG. 13: (Color online) Data for ξ_{CG}/N , the chiral glass correlation length divided by system size, as a function of T for different system sizes, for $\sigma = 1.0$. The inset is a log-log fit to the intersection temperatures $T^*(N, 2N)$, assuming $T_{CG} = 0$. The data is quite consistent with this behavior.

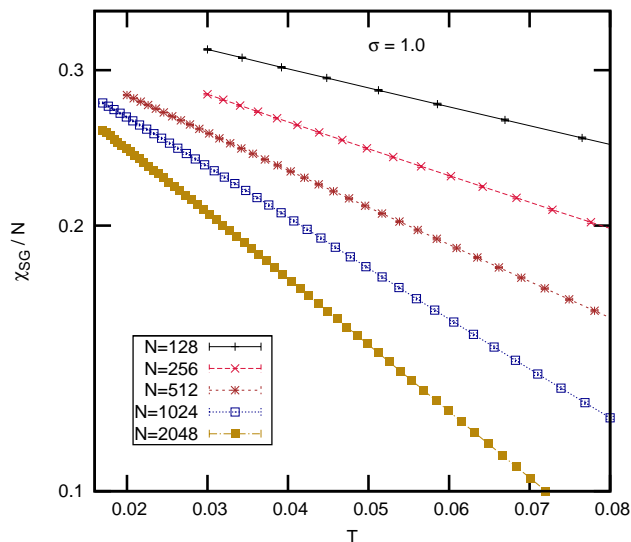


FIG. 14: (Color online) Data for χ_{SG}/N , the spin glass susceptibility divided by system size (the power $2-\eta$ is equal to 1 here), as a function of T for different system sizes for $\sigma = 1.0$. There are no intersections for the temperature-range in which the simulation is conducted.

V. CONCLUSIONS

Our primary motivation to study the Heisenberg spin glass in one dimension with long-range interactions which fall off with the power of the distance, is to test Kawamura's spin-chirality decoupling scenario in which $T_{CG} > T_{SG}$, and his subsequent prediction²⁰ that chiral glass or-

dering persists for $\sigma > \sigma_l$, where $\sigma_l = 1$ is the “lower critical” value for the spin glass transition, with a finite value of T_{CG} at $\sigma = 1$.

For $\sigma = 1$ we find $T_{CG} = T_{SG} = 0$ in contrast to Viet and Kawamura²⁰. For most of the other values of σ our data is well consistent with a single phase transition.

However, for $\sigma = 0.85$ the best fits for the sizes we can equilibrate indicate $T_{CG} > T_{SG}$, see Fig. 9. Interestingly that figure shows very strong subleading corrections to finite-size scaling in the data for ξ_{SG} since it only fits Eq. (23) for the largest sizes. At intermediate sizes the intersection temperatures seem to be heading towards the chiral glass transition temperature obtained from the ξ_{SG} data, but then dip down for the largest sizes. We therefore cannot rule out that similar behavior might occur for the chiral glass correlation length but at even larger length scales. In this case there would be no spin-chirality decoupling. We also note that, for a given size and temperature, ξ_{CG} remains considerably smaller than ξ_{SG} in the vicinity of the intersection temperatures T^* , compare the main part of Fig. 7 with Fig. 8. Hence the data is very far from the regime with $\xi_{CG} > \xi_{SG}$ which ultimately prevails for $T_{SG} < T < T_{CG}$ if there is spin-chirality decoupling.

In a subsequent paper²¹, we will investigate, for the same models, under what circumstances an AT line of transitions occurs in a magnetic field.

Acknowledgments

We acknowledge support from the NSF under Grant DMR-0906366. AS also acknowledges partial support from DOE under Grant No. FG02-06ER46319.

-
- * Electronic address: peter@physics.ucsc.edu
- ¹ F. Dyson, *Communications in Mathematical Physics* **12**, 212 (1969).
 - ² F. Dyson, *Communications in Mathematical Physics* **21**, 269 (1971).
 - ³ G. Kotliar, P. W. Anderson, and D. L. Stein, *Phys. Rev. B* **27**, 602 (1983).
 - ⁴ H. G. Katzgraber and A. P. Young, *Phys. Rev. B* **72**, 184416 (2005).
 - ⁵ H. G. Katzgraber, D. Larson, and A. P. Young, *Phys. Rev. Lett* **102**, 177205 (2009), (arXiv:0812:0421).
 - ⁶ L. Leuzzi, G. Parisi, F. Ricci-Tersenghi, and J. J. Ruiz-Lorenzo, *Phys. Rev. Lett* **101**, 107203 (2008).
 - ⁷ M. A. Moore, *Phys. Rev. B* **82**, 014417 (2010).
 - ⁸ L. Leuzzi, G. Parisi, F. Ricci-Tersenghi, and J. J. Ruiz-Lorenzo, *Phys. Rev. Lett* **103**, 267201 (2009).
 - ⁹ H. Kawamura and M. Tanemura, *Phys. Rev. B* **36**, 7177 (1987).
 - ¹⁰ K. Hukushima and H. Kawamura, *Phys. Rev. E* **61**, R1008 (2000).
 - ¹¹ K. Hukushima and H. Kawamura, *Phys. Rev. B* **72**, 144416 (2005).
 - ¹² F. Matsubara, T. Shirakura, and S. Endoh, *Phys. Rev. B* **64**, 092412 (2001).
 - ¹³ S. Endoh, F. Matsubara, and T. Shirakura, *J. Phys. Soc. Jpn.* **70**, 1543 (2001).
 - ¹⁴ T. Nakamura and S. Endoh, *J. Phys. Soc. Jpn.* **71**, 2113 (2002), (arXiv:cond-mat/0110017).
 - ¹⁵ M. Picco and F. Ritort, *Phys. Rev. B* **71**, 100406(R) (2005).
 - ¹⁶ L. W. Lee and A. P. Young, *Phys. Rev. Lett.* **90**, 227203 (2003), (arXiv:cond-mat/0302371).
 - ¹⁷ L. W. Lee and A. P. Young, *Phys. Rev. B* **76**, 024405 (2007), (arXiv:cond-mat/0703770).
 - ¹⁸ I. Campos, M. Cotallo-Aban, V. Martin-Mayor, S. Perez-Gaviro, and A. Tarancon, *Phys. Rev. Lett.* **97**, 217204 (2006), (arXiv:cond-mat/0605327).
 - ¹⁹ L. A. Fernandez, V. Martin-Mayor, S. Perez-Gaviro, A. Tarancon, and A. P. Young, *Phys. Rev. B* **80**, 024422 (2009), (arXiv:0905.0322).
 - ²⁰ D. X. Viet and H. Kawamura, *Phys. Rev. Lett.* **105**, 097206 (2010), (arXiv:1004.3170).
 - ²¹ A. Sharma and A. P. Young, (unpublished).
 - ²² J. R. L. de Almeida and D. J. Thouless, *J. Phys. A* **11**, 983 (1978).
 - ²³ A. Sharma and A. P. Young, *Phys. Rev. E* **81**, 061115 (2010), (arXiv:1003.5599).
 - ²⁴ J. R. L. de Almeida, R. C. Jones, J. M. Kosterlitz, and D. J. Thouless, *J. Phys. C* **11**, L871 (1978).
 - ²⁵ H. G. Katzgraber and A. P. Young, *Phys. Rev. B* **67**, 134410 (2003).
 - ²⁶ D. Sherrington and S. Kirkpatrick, *Phys. Rev. Lett.* **35**, 1792 (1975).
 - ²⁷ G. Parisi, *Phys. Rev. Lett.* **43**, 1754 (1979).
 - ²⁸ G. Parisi, *J. Phys. A* **13**, 1101 (1980).
 - ²⁹ G. Parisi, *Phys. Rev. Lett.* **50**, 1946 (1983).
 - ³⁰ T. Mori, (unpublished).
 - ³¹ T. Mori, *Phys. Rev. E* **82**, 060103(R) (2010).
 - ³² H. G. Katzgraber, M. Palassini, and A. P. Young, *Phys. Rev. B* **63**, 184422 (2001), (arXiv:cond-mat/0007113).
 - ³³ J. Alonso, A. A. Tarancón, H. Ballesteros, L. Fernández, V. Martín-Mayor, and A. Muñoz Sudupe, *Phys. Rev. B* **53**, 2537 (1996).
 - ³⁴ J. Pixley and A. P. Young, *Phys. Rev. B* **78**, 014419 (2008).
 - ³⁵ K. Hukushima and K. Nemoto, *J. Phys. Soc. Japan* **65**, 1604 (1996), (arXiv:cond-mat/9512035).
 - ³⁶ E. Marinari, in *Advances in Computer Simulation*, edited by J. Kertész and I. Kondor (Springer-Verlag, 1998), p. 50, (arXiv:cond-mat/9612010).
 - ³⁷ For a discussion of how finite-size scaling is modified in the region of mean-field exponents, see for example Refs. [43–47].
 - ³⁸ K. Binder, *Z. Phys. B* **43**, 119 (1981).
 - ³⁹ H. G. Ballesteros, L. A. Fernandez, V. Martin-Mayor, J. Pech, and A. Muñoz Sudupe, *Phys. Lett. B* **387**, 125 (1996), (arXiv:cond-mat/9606203).
 - ⁴⁰ M. Hasenbusch, A. Pelissetto, and E. Vicari, *Phys. Rev. B* **78**, 214205 (2008), (arXiv:0809.3329).
 - ⁴¹ D. Larson, H. G. Katzgraber, M. A. Moore, and A. P. Young, *Phys. Rev. B* **81**, 064415 (2010), (arXiv:0908.2224).
 - ⁴² W. H. Press, S. A. Teukolsky, W. T. Vetterling, and B. P. Flannery, *Numerical Recipes in C, 2nd Ed.* (Cambridge University Press, Cambridge, 1992).
 - ⁴³ E. Brézin, *J. Phys. (Paris)* **43**, 15 (1982).
 - ⁴⁴ E. Brézin and J. Zinn-Justin, *Nucl. Phys. B* **257**, 867 (1985).
 - ⁴⁵ K. Binder, M. Nauenberg, V. Privman, and A. P. Young, *Phys. Rev. B* **31**, 1498 (1985).
 - ⁴⁶ E. Luijten, K. Binder, and H. W. J. Blöte, *Eur. Phys. J. B* **9**, 289 (1999).
 - ⁴⁷ J. L. Jones and A. P. Young, *Phys. Rev. B* **71**, 174438 (2005), (arXiv:cond-mat/0412150).